Accepted Manuscript

Ionospheric precursors of earthquakes and Global Electric Circuit
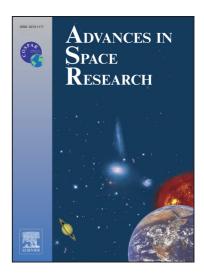
Sergey Pulinets, Dmitry Davidenko

ADVANCES IN
SPACE
RESEARCH

ISSN: 0273-1177

Ionospheric precursors of earthquakes and Global Electric Circuit

Sergey Pulinets[1], Dmitry Davidenko[2]

[1]Space Research Institute, Russian Academy of Sciences, Moscow, Russia
[2]S.P. Korolev Rocket and Space Corporation «ENERGIA», Korolev, Russia

pulse@rssi.ru

Abstract

The electromagnetic coupling between the seismically activated area and the ionosphere is considered within the framework of the Global Electric Circuit (GEC) conception. First we consider the anomalous variations in the ionosphere associated with the earthquake preparation process, their temporal and spatial characteristics using the results from recent publications. Then the GEC conception is presented shortly with main accent put on ionization processes which play key role in the complex chain of physical and chemical interactions changing the electric properties of the planetary boundary layer of atmosphere. We treat this part of troposphere as an open complex system with dissipation where so called "blow up" processes are developed leading to sharp and fast changes of atmospheric parameters including the electric properties of the boundary layer. The new concept named Spatial Scintillation Index is introduced in the last part of the paper. In general, this paper may be considered as a short review of the recent achievements in understanding of the seismo-ionospheric coupling.

1. Introduction

The history of seismo-ionospheric effects and ionospheric anomalies observed over the earthquake preparation zone counts more than 50 years. Its early stages of development are described in (Pulinets and Boyarchuk, 2004). If to summarize the main trend – it is the smooth transition from acoustic-driven mechanisms to the electromagnetic coupling. The reason of this is very simple: acoustic coupling mechanism has shown recently its very low effectiveness – effects from giant Sumatra 2004 and Tohoku 2011 tsunamis was so weak: 0.1 – 0.4 TECU for Sumatra tsunami (Liu et al., 2006a; Astafieva and Afraimovich, 2006); and 0.5 – 1.5 TECU units for Tohoku tsunami (Galvan et al., 2012), that it is difficult to expect that before earthquakes happens something stronger what can produce

an order of magnitude larger variations in the ionosphere which are really observed before earthquakes. Another argument is that Acoustic Gravity Wave (AGW) driven ionospheric disturbance should have wave-like structure and should move with velocity of sound while pre-seismic ionospheric anomalies have persistent character and do not show any tendency of movement: they are stationary in space. So further in the paper only electromagnetic driven ionospheric disturbances associated with earthquakes will be discussed.

The very early versions of seismo-ionospheric coupling models were based on direct calculations of seismogenic electric field effect from the ground surface to the ionosphere (Kim et al., 1994; Pulinets et al., 1998a, Pulinets et al., 2000). All of them are based on the methodology of electric field penetration into the ionosphere from thundercloud (Park and Dejnakarintra, 1973). The most recent version of this approach one can find in (Kim et al., 2012) where anisotropy of the ionospheric conductivity is taken into account more correctly than in previous publications. But this approach is insufficient from several points of view: a) it does not consider the nature of anomalous seismogenic electric field; b) it does not work at equatorial latitudes; c) it takes as an initial condition the minimal value of the vertical electric field at the ground surface no less than 1000 V/m what is observed not so often, while the ionospheric anomalies are registered regularly, including the anomalies over the sea surface (Li and Parrot, 2013).

Next trend in electromagnetic coupling of ground and ionosphere before earthquakes is the arbitrary introducing of the electric currents and fields at different altitudes (Sorokin, 2007; Kuo et al., 2011; Namgaladze et al., 2012; Klimenko et al., 2011). Sorokin (2007) as a driver for his coupling mechanism introduces the external current which is generated by charged aerosols possibly injected into atmosphere within the seismically active zones. There are two major difficulties which every reader encounter dealing with this conception: a) there is no any scientific publication demonstrating such injection of charged aerosols into atmosphere before earthquakes; b) the value of the vertical external current introduced by the author is $4 \cdot 10^{-6}$ A/m^2 which is six orders of magnitude larger than the natural fair weather current flowing in the Global Electric Circuit what is absolutely impossible. Introducing this current it should be taken into account what happens with the air conductivity at different altitudes, what is vertical gradient of atmospheric electric field. No one of these questions find the answer in the publications of Sorokin. If these fluxes of aerosols existed, they could be injected only over the land, and no ionospheric effect over the ocean would be

observed what comes into contradiction with the recent DEMETER satellite data (Li and Parrot, 2013). Regardless the very high quality 3-D mode calculations presented in the paper (Kuo et al., 2011) it can be criticized from the same position as the paper of Sorokin (2007). As the source of external current the authors use the stress-activated p-hole rock conductivity (Freund, 2010). Their arbitrary source is even much more different from the value of the natural fair weather current ($4 \cdot 10^{-12}$ A/m^2) and varies from 0.1 μA/m^2 till 10 μA/m^2. It means that even smallest current density used in their model is 5 orders of magnitude larger than the natural value. The same comment could be applied to the current source: if this mechanism is valid, it is possible only over the land, what again contradicts with the modern experimental data. In addition p-holes have the positive charge, and it means that the only one sign of deviation from the undisturbed value of electron concentration can be induced in the ionosphere, while we observe experimentally both negative and positive variations of plasma concentration in the ionosphere before earthquakes.

At the same time it should be noticed that all recent calculations (Klimenko et al., 2011; Kuo et al., 2012; Namgaladze et al., 2012) agree in one principal thing, that the zonal electric field in ionosphere of the order of several mV/m can create anomalies similar to registered experimentally, and all three models introducing the zonal electric field at ionospheric heights perfectly reproduce the morphology of seismo-ionospheric variations. This fact immediately generates the request for the physical mechanism which is able to produce such fields in the ionosphere at the last stage of earthquake preparation cycle. Such idea was proposed by Pulinets (2009). It is not the model yet because there are no real calculations, especially of penetration the anomalous electric field from 60 km (altitude considered as the ionospheric layer responsible for atmosphere-ionosphere coupling in GEC to the upper ionospheric altitudes), but this paper shows direction where our attempts should be directed to, and this is the breakthrough direction of ionospheric physics not only from the point of view of seismo-ionospheric coupling, but in the atmosphere-ionosphere coupling in general.

2. How look seismo-ionospheric pre-earthquake variations and their main characteristics

Ten years passed from the first attempt to generalize information on the main characteristics of pre-earthquake variations in the ionosphere (Pulinets et al., 2003) for the modern science is enormous period from many points of view.

Instead of several small groups of enthusiasts ten years ago, now the majority of institutions dealing with ionospheric physics try in some manner to be involved in these studies. And announced recently by ESA Invitation to Tender AO/1-7548/13/NL/MV "Ionospheric Sounding for Identification of Pre-Seismic Activity" demonstrates that governmental bodies also take the problem seriously.

Comparing from 15 years back studies, in addition to results of the vertical ground based and topside sounding and some limited information from the satellite local probes we have now plenty of data from GPS TEC measurements (Xia et al., 2011), low orbit and high orbit ionospheric tomography (Hirooka et al., 2011; Kunitsyn et al., 2012), occultation measurements from satellites (Hsiao et al., 2010), and 6 years in orbit the purpose-directed satellite DEMETER with many different space probes and wave measurements (Li and Parrot, 2013). In these conditions we can claim that we know almost everything on this phenomenon, including the statistics gathered by different researchers (Le et al., 2011; Li and Parrot, 2013). We will consider the main features of ionospheric precursors using the ordinary procedure of ionospheric variability estimation. One should keep in mind that the parcel of ionospheric plasma takes place simultaneously in different types of variability: temporal, spatial, altitude, etc., but to systemize in some way the main features of seismo-ionospheric variations we examine them by traditional way. It should be mentioned also that to not repeat earlier publications (Pulinets et al., 1998b; Pulinets et al., 2003; Pulinets and Boyarchuk 2004) we will make accent on new findings.

2.1. Temporal variability of ionospheric precursors.

It is accepted in ionospheric physics that ionospheric variability is usually measured as deviation from monthly median (Bradley and Cander, 2002). Taking into account that studies of ionospheric precursors have applicative character, and final purpose of these studies is the short-term forecast, usually the running 15-day median (or mean for GPS TEC) is calculated for 15 days preceding the day of consideration (Liu et al., 2006b). It is established that there are observed both the positive and negative deviations from undisturbed level but what was revealed recently that they are not sporadic, and have regular character in relation to the day of earthquake and this dependence has the physical meaning (Pulinets, 2012) what will be explained lower. Wenchuan earthquake is a good example of such variations. In Fig. 1 (Liu et al., 2011) one can see the clear negative deviation of GPS TEC on 6 May, and then clear positive deviation on 9 of

May before the deadly M7.9 earthquake on 12 May. This tendency was confirmed by the GPS TEC mapping of earthquake effects in the ionosphere around the time of 3 strong (M > 7.0) earthquakes occurred in Qinghai-Tibet region (Xia et al., 2011).

If we look inside the specific day when the precursory variations were detected, we discover that their emerging is also not random and happens during the same interval of the local time, specific for different seismic zones (Pulinets et al., 1998b). In Taiwan it happens usually in afternoon hours (Liu et al., 2006b), but in Greece, for example, we can observe the positive deviation lasting 12 hours from 4 PM till 4 AM (Ouzounov et al., 2013; Davidenko, 2013). The possible reasons of local time dependence of ionospheric precursors will be discussed lower.

If to consider the next temporal parameter of ionospheric precursors – time duration, we should update the statement from earlier paper (Pulinets et al., 2003) where we claimed that their duration is near 4 hours to more extended period: Ionospheric precursors may last from 4 to 12 hours, and can repeat the same variations several days by order.

The last temporal characteristic of ionospheric precursors which should be mentioned, it is the leading time of precursors emerging before the seismic shock. From the very early publications (Pulinets, 1998), its value did not changed essentially. As statistical studies show using different techniques (ground based vertical sounding, GPS TEC, GIM maps) all techniques, even extensive in time and very sophisticated statistical processing (Liu et al., 2006b) give the average value 5 days before the seismic shock. The most convincing result was presented recently by Michel Parrot at the 2012 Fall Session of American Geophysical Union (Parrot and Li, 2012) where the same 5 days were revealed after processing of ionospheric anomalies registered over 5742 earthquakes while passing of DEMETER over earthquake preparation area. It is important to note, that the same 5 days leading time interval is revealed from statistical studies of other types of earthquake precursors: OLR (Outgoing Longwave infrared Radiation (Ouzounov et al., 2012), anomalies of subionospheric VLF radiowave propagation over earthquake preparation area (Hayakawa et al., 2010), and even dragging/deceleration of small satellites in the upper ionosphere over the earthquake preparation zones (Tertyshnikov et al., 2009). It implies that there exists some periodicity during the last stage of the seismic cycle. Applying more severe criteria for the seismo-ionospheric anomalies selection (Le et al., 2011)

makes the leading time interval shorter for smaller and deeper earthquakes but still the limiting time for them statistically confident remains 5 days (see Fig. 2).

The leading time of ionospheric precursors (near 5 days) gives us the instrument to estimate the time of impending earthquake in the case of forecast.

2.2. Spatial characteristics of ionospheric precursors

To the spatial characteristics we attribute the position of ionospheric anomaly in relation to the vertical projection of impending earthquake epicenter, the size of anomaly, and its relation with the earthquake magnitude. The very important factor is so called spatial scintillation of electron concentration over the area of earthquake preparation. Special paragraph will be devoted to this phenomenon.

Taking into account the physical nature of ionospheric precursors which is associated with air ionization produced by radon (Pulinets and Boyarchuk, 2004) it should be quite natural that spatial distribution of anomaly in the ionosphere should follow the radon anomalies distribution on the ground surface. As extensive geochemical investigations have been demonstrated (Toutain and Baubron, 1998), radon is following the Dobrovolsky relationship between the size of earthquake preparation zone and earthquake magnitude (Dobrovolsky et al., 1979). This relationship looks like:

$$R=10^{0.43M} \tag{1}$$

where R – radius of the earthquake preparation zone in km, M – earthquake magnitude by Richter scale. Similar relationship was derived by Bowman et al. (1998), but with index 0.44 before M, and the authors name this region as "earthquake activation zone". If the proposed mechanism is correct, it is quite natural to expect the size of anomaly in the ionosphere at least of the same order of magnitude. In the top panel of the Fig.3 one can see the latitudinal cross-section of deviation of the critical frequency scaled from topside sounder ionograms of the Intercosmos-19 satellite passing over the preparation zone of the Irpinia M6.9 earthquake of 23 Nov. 1980 in Italy 2.5 days before the seismic shock (Pulinets et al., 2007a). It is seen that anomaly is formed in both North and South hemispheres demonstrating magnetically conjugated effect. Estimating diameter of the modified region in the northern hemisphere (near 1800 km) one can estimate the magnitude of impending earthquake using the relationship (1):

$$M=[\log(1800/2)]/0.43 = 6.9 \tag{2}$$

what is exactly the Irpinia earthquake magnitude. In the bottom part of Figure 3 the differential GIM map is shown built by Liu et al. (2010) for time interval before the Andaman-Sumatra M9.3 26 Dec 2004 earthquake, on 21 December, 5 days before the main shock. It is important to note that anomaly should not necessary to fill all area of earthquake preparation, but what is interesting, it is perfectly inscribed in the circle of Dobrovolsky.

In comparison with the early stage of ionospheric precursors' studies, recent results demonstrate the strong dependence of the ionospheric precursors spatial characteristics on latitude. Ionospheric anomalies demonstrate strong longitudinal variations for the low latitude earthquakes (Pulinets, 2012). As concerns the middle latitudes, precursors demonstrate the equatorward shift from the vertical projection of epicenter (Pulinets et al, 2007). All modelers who are able to reproduce the TEC anomalies before earthquakes (Namgaladze et al., 2009; Klimenko et al., 2011; Zolotov et al, 2012) need anomalous zonal electric field in the ionosphere. The physical mechanism showing how this field can be generated was proposed in (Pulinets, 2009; Pulinets, 2012). Generally speaking, in low latitudes we usually observe longitudinally elongated anomaly to the east and to the west from epicenter, and for middle latitude earthquakes we observe spot of positive or negative deviation centered over epicenter or shifted equatorward what is shown in the Figure 4.

To conclude this paragraph it should be underlined that the locality of ionospheric precursors is one of the main features used for their identification. Solar and geomagnetic activity lead to global variability in the ionosphere while final stage of earthquake preparation produce variations only over the earthquake preparation zone what gives us in hands the instruments for estimation of the position of impending earthquake epicenter and its magnitude (the second from 3 parameters necessary for earthquake forecast).

2.3. Altitude distribution of ionospheric precursors

We will consider precursors phenomena in different layers of the ionosphere and especially the modification of the vertical profile of electron concentration in the F-region of the ionosphere.

Subionospheric propagation of the VLF waves – is one of the most sensitive techniques of the D-region variability. It was found that the changes of atmosphere conductivity due to particle precipitation (Kim et al., 2002) or due to

radioactive pollution and subsequent air ionization (Fux et al., 1997) lead to effective lowering of the D-region what creates anomalous effects in the VLF wave propagation. In case of earthquake preparation the increased level of radon emanation within the area of earthquake preparation changes the conductivity of the boundary layer of atmosphere – the lower part of the Global Electric Circuit vertical conductivity. In Europe, Russia and Japan is created the monitoring network able to detect the pre-earthquake effects in the VLF wave propagation few days before the seismic shock (Hayakawa et al., 2010, Rozhnoi et al., 2012).

The regular E-region of the ionosphere is well controlled by the solar radiation, and it is difficult to expect some significant anomalies created by the earthquake preparation during the daytime. But in night-time conditions it is possible to expect the variations of electron concentration in the regular E-layer (Pulinets et al., 1998a). Nevertheless, the sporadic E-layer is much more sensible to any variations, especially to electric fields which can create the anomalous E_S-layers (Pulinets et al., 2000). Intensification of E_S activity before earthquakes is reported in the literature (Liperovsky et al., 2005). One of the manifestation of increased E_S activity is the excess of foE_S over the $foF2$ during earthquake preparation period. In the Figure 5 one can see such effect during period of Kultuk earthquakes near Baykal Lake in August 2008 when two moderate shocks took place with M 5.7 on 16 Aug 2008 and M6.3 on 27 Aug 2008. Critical frequency of E_S-layer is shown by blue color, and $foF2$ – by red color. The days of earthquakes are indicated by red arrows in the top. One can clearly see that the foE_S systematically exceeds $foF2$ until the second shock, after which the E_S activity disappears.

Rising to the altitudes of F2-layer we should mention the very interesting effect which is not considered in modern publications on the ionospheric precursors because of absence of topside sounders in the orbit, and as a consequence – inability to measure the shape of topside profile. The regular increase of scale-height of topsides profiles before earthquakes was reported in (Pulinets and Boyarchuk, 2004). This effect was interpreted as increase of concentration of the light ions at the altitudes with prevailing concentration of O^+ ions and effective decrease of the mean ion mass. IAP (Ion Analyzer Probe) on the DEMETER satellite was able to measure the concentration of mean ions of the ionosphere at the orbit altitude. So the increased concentration of light ions before strong earthquakes could confirm the result obtained with the help of topside sounder. In the Figure 6a one can see the increased concentration of H^+ ions during several days while passing the DEMETER satellite over the area of Wenchuan earthquake

preparation (Zhang et al., 2009). Pulinets et al. (2010) using the technique developed by Smirnov (2001) of the vertical profile reconstruction from GPS TEC data demonstrated the increase of the topside profile semi-thickness few days before the same Wenchuan earthquake (Figure 6b). Together with temperature variations the scale height and ion composition are important factors to identify the ionospheric precursors because their morphology is quite different from the same parameters variations during the geomagnetic storms (Pulinets and Boyarchuk, 2004).

3. Global Electric Circuit as a principal means for atmosphere-ionosphere coupling

Recent years are characterized by intensification of research on the Global Electric Circuit (GEC) conception explaining the mechanism of generation of the vertical atmospheric electric field and creation of the potential difference between the ground and lower boundary of ionosphere (near 60 km altitude): (Markson, 2007; Williams, 2009; Mareev, 2010; Rycroft et al., 2012). To get more comprehensive understanding of this conception I recommend to look at the papers cited above. Here we will concern only on one specific effect – impact of the radioactivity and radiative ionization on the parameters of the Global Electric Circuit.

Due to thunderstorm activity and electrified convective clouds which could be considered as electric generators the ionosphere acquires the positive potential from 200 till 500 kV in relation to the ground surface. It was discovered that during period of nuclear weapon tests in atmosphere the ionospheric potential (Vi) undergo essential variations (Markson, 2007) which are shown in the Figure 7. Two segments of the curve showing the multi-year variations of ionospheric potential are selected by red circles: the first one – increase of the ionospheric potential during period of intensive nuclear weapon tests in atmosphere, and the second circle –drop of ionospheric potential as a reaction on Chernobyl atomic power plant accident in 1986. To clarify this, we should look at the processes of radiative ionization in atmosphere and its consequences.

3.1. Radiative ionization effects on atmosphere conductivity

Ionization potentials of atmospheric gases are very low: from 9.5 eV (NO) to 24.6 eV (He$_2$). At the same time, decay energy of different elements appearing during nuclear explosion is much higher (^{90}Sr – 0.546 MeV, its secondary product

^{90}Y – 2.28 MeV, ^{131}I – from 0.248 to 0.807 MeV); the main source of the natural radioactivity ^{222}Rn emits α-particles with energy 5.59 MeV. It means that all sources of radioactivity through impact ionization can produce large amount of ions (positive and negative). These primary ions can interact in different plasma-chemical reactions and form more complex secondary ions. Main reactions were considered in (Pulinets and Boyarchuk, 2004). And after that another very powerful and exothermic reaction takes place – ions' hydration – free water molecules existing in air attach to new formed ions. All this together now is called Ion Induced Nucleation (Kathmann et al., 2005). Depending on ambient conditions the different size particles can be formed, including the aerosol size (Tammet and Kulmala, 2005). We should keep in mind that all these particles are still charged, i.e. they contribute into the atmosphere conductivity with different sign. If light ions increase the atmosphere conductivity, the heavy ions decrease it because of their low mobility, what is more, mobility can differ more than 3 orders of magnitude. Looking at the formula of air conductivity:

$$\sigma = e\sum_{i=1}^{n}\left(n_i^+ \mu_i^+ + n_i^- \mu_i^-\right) \tag{3}$$

where n_i^+ and n_i^- - concentration of positive and negative ions of different kinds, μ_i^+ and μ_i^- mobilities of positive and negative ions.

If we return to the Figure 7, we can see within the first circle the negative peaks of ionospheric potential which testify the drop of ionospheric potential due to conductivity increase. But accumulation of ^{90}Sr both in atmosphere and ground surface with increased number of tests transformed the process of ionization from transient to permanent and to accumulation of so called "aged" heavy ions decreasing the atmosphere conductivity and increasing the ionospheric potential Vi. In the case of Chernobyl due to atmospheric conditions the radioactive substances spread over the planet and led to increase of atmosphere conductivity and to decrease of ionospheric potential.

3.2. Independent check of relation between the air conductivity and possible effects in the ionosphere

Nature and human activity provides us other sources of the local sharp transient changes of air conductivity. Volcano eruptions are one of the most outstanding natural phenomena affecting the human life. The huge amounts of volcanic ash

emitted into the atmosphere create the layer of very low conductivity at the altitude of 5-15 km. Can the layer of decrease conductivity affect the whole resistivity of atmosphere? Let us look at simplified schematic diagram of the GEC (Figure 8). We can conditionally present the total air electric resistance by three main components: stratosphere R_S, troposphere R_T, and lower boundary layer R_{BL}, which is actually the part of troposphere, but very specific part containing up to 75% of the total columnar resistance of the atmosphere (Hoppel, 1986). Due to series connection of resistors the resistance of the boundary layer plays the role of the electric current limiting resistor. Its variations will strongly affect the total columnar resistance, and hence, the ionospheric potential Vi.

Returning to volcano eruption, we can state that introducing the low conductivity layer of volcanic ash, we drastically increase the total columnar resistance of atmosphere, and hence, increase the ionospheric potential. What will happen with electron concentration in the ionosphere? In the left panel of the Figure 9 is shown the spatial distribution of ash on 16 of April 2010 after eruption of the Island volcano Eyjafjallajökull (BBC News, 2010), and at the right panel – the differential TEC maps build using the IGS GIM. The positive deviation is not so large (near 3 TEC units) but it is probably due to the fact that the ash layer was at relatively high altitudes (near tropopause) which contribution to the column resistance is smaller than the boundary layer.

The second test was done using the data collected during the Western Africa dust storm 29 Apr – 1 Jun 2012. We don't have the direct measurements of the air conductivity for this specific storm but there are historical data (Gringel and Mühleisen, 1978) of the balloon measurements of atmosphere vertical profile of conductivity 2200 km from Western Africa in Atlantics during Sahara dust storm, (see left panel of the Figure 10) when the essential drop of air conductivity was registered. The time series of differential TEC maps show much more essential relative TEC increase, up to 10 TEC units. It is connected with the fact that for the dust layer is on much lower altitudes than the volcanic ash: 2-3 km.

From these two examples we can conclude that the drop of atmosphere conductivity (what is equivalent to the column resistance increase) leads to appearance of the local positive TEC anomalies.

It would be interesting to check the opposite case: local increase of atmosphere conductivity. Usually such effects are connected with the nuclear explosions: intended nuclear tests or emergency situations on the atomic power plants. We

were able to register one of the recent events: underground nuclear test in Northern Korea on February 12, 2013 (Figure 11). Because of underground explosion, effect was very weak (mainly due the leakage), nevertheless, it shows the clear negative deviation, but the radioactive cloud due to the North-West wind is shifted to the Honshu Island.

Finalizing this paragraph we can conclude that the sharp local increases of the column conductivity lead to the decrease of electron concentration over the modified area, and decreases of conductivity – the positive effects in the ionosphere.

3.3. Natural ground radioactivity and earthquakes

In the case of earthquakes all ionization processes start near the ground surface where increased radon emanation from the active tectonic faults rapidly increases the boundary layer conductivity. But because of the track-like character of ionization produced by α-particles (Pulinets and Boyarchuk, 2004), the ion concentration inside the tracks becomes very high (up to 10^6-10^7 cm^{-3}). Such high level of ion concentration lead to explosive nucleation processes and formation of ion clusters with size of several microns (Pulinets and Ouzounov, 2011) which will drastically decrease the air conductivity.

The question is often appeared: what about the ocean? We see the same kind of anomalies over the ocean surface. What is the ionization source there? You will be surprised but it is radon again. First of all one should keep in mind that the main way of radon from the crust into the atmosphere is not its own diffusion but the participation in common gas migration process (Khilyuk et al., 2000) where the carbon dioxide and methane play role of main carriers of radon to the ground and ocean surface (one can call to mind the videos of Deep Water Horizon oil platform disaster in Mexican Gulf in 2010 where the huge bubble of methane was the reason of explosion). And there are plenty of publications of radon measurements over ocean surface where radon is used as a trace gas to evaluate the carbon dioxide fluxes from the ocean (Kawabata et al., 2003).

If to consider the development of ionization effect in time, we may expect first the negative deviation of electron concentration in the ionosphere over the seismically active area on initial stage of sharp radon flux increase, and then, with development of nucleation, – the positive effect. Let us return to the Figure 1 of this manuscript, and we immediately will see this effect of TEC deviation

registered before the Wenchuan earthquake. Because of close proximity of equatorial anomaly, the situation of TEC variability around the time of the Wenchuan earthquake is more complex (it necessary to consider the longitudinal effect from west and from east of impending epicenter position), but because the lack of place in present publication, the detailed analysis of this case one can find in (Pulinets, 2012). It should be noted that the recent Lushan M7 earthquake on 20 April 2013 in China (very close to the Wenchuan earthquake) the ionospheric effects are very similar to those before the Wenchuan earthquake what confirms the hypothesis on the similarity of the ionospheric effects before earthquakes in the same geographic region.

4. Spatial Scintillation Index as one of the most reliable means to identify ionospheric precursors

There are some traps in data analysis when using the time series. It is very difficult to distinguish between the temporal variations of parameter in the given point and spatial changes (for example when satellite is moving along its orbit). Sometimes simplified analysis leads to the wrong conclusions what happened with the authors of the papers (Thomas et al., 2011, and Masci, 2013). These papers are commenting our previous publication (Pulinets et al., 2007b) where so called Local Variability Index was introduced. In their analysis they interpret the variability of this index as time series forgetting that it combines the data of GPS receivers distributed in space within the area of earthquake preparation. It was discovered in publication of 2007 that during geomagnetic disturbances the cross-correlation coefficient of daily variations of TEC between the neighboring stations growth, demonstrating that the electric fields triggered by the geomagnetic disturbance work as driving forces in mechanics of forced oscillations. While before the earthquake the cross-correlation drops. What is the reason of this phenomenon? If we look at the system of activated tectonic faults before earthquake using the images of land surface thermal anomalies (Li et al., 2011) we can see very irregular picture of linear anomalies associated with faults, like it was registered before the Wenchuan earthquake (Figure 12). One should keep in mind that these thermal anomalies are also result of ionization produced by radon, and nucleation producing the release of latent heat –the source of the thermal anomalies (Pulinets and Ouzounov, 2011). One may expect that air conductivity will be changed not evenly in space but will be similar to some

scintillations following the tectonic faults activity. It means that the ionospheric potential will demonstrate spatial scintillations following this irregular structure of air conductivity. Now, if we try to study the spread in TEC data collected within the area of this air conductivity irregularity, we will observe the difference in receiver readings even situated close one to another. And this is the sense of the introduced index. The authors of the papers cited above and criticized our approach interpreted this index like one-point parameter, and this led them to the wrong conclusions.

Now we will try to demonstrate this visually. In the Figure 13a are shown in the upper panel the introduced index, and the lower panel – the equatorial Dst index for the period around the time of the Hector mine M7.1 earthquake on 16 Oct 1999 in California. In the bottom panel one can see two periods of increase geomagnetic activity almost identical. We can say that the second period is even more active because of the strong geomagnetic storm 22 of October. Nevertheless, the index variations are stronger before the seismic shock marked by black arrow in the top panel, than during the second activity period. What is the reason? The answer is shown in the Figure 13b where the spatial distribution of GPS TEC is shown for the same values of Dst during the first geomagnetically active period (left) and during the second one (right). In the left panel one can see the rough surface with large spread in TEC values over the area, while in the right one we see the flattish plane. Without the earthquakes this plane is moving up and down, even during the geomagnetic storm, while before the earthquakes we will see the washboard-like spatial distribution. To avoid the further mistakes in interpretation of the discussed index we propose here to rename it from Local Variability Index to the Spatial Scintillation Index (SSI).

We calculate this index now for every major earthquake where the local GPS TEC data are available, and some examples are shown in the Figure 14. As some improvement we calculate now the daily variations which show more smoothed data (Figure 14c). From top to bottom one can see: SSI calculated for period of 4 months before and during Sumatra Andaman M9.1 earthquake on 26 Dec 2004, Chile M8.8 earthquake on 27 Feb 2010, and L'Aquila M6.3 earthquake on 6 Apr 2009. The last one presented as daily SSI. There are similarities and difference in the SSI behavior: the most active was period around the time of Chile earthquake, the index started to increase 10 days before the earthquake and was active 20 days after due to the high aftershock activity. But both Mega and moderate earthquake demonstrate the increase of the SSI a few days before the seismic

shock. One important remark should be made here. The stations used for SSI calculations should be in the same ionospheric conditions. What does it mean? For example for Sumatra case were selected receivers between the crests of equatorial anomaly because if to take one station in the trough, and one – in the crest – they obviously will show quite different behavior.

5. Conclusion

It was almost impossible task to put together in one paper the all information on ionospheric precursors of earthquakes which we were able to collect for the present moment. So decision was made to demonstrate the most remarkable features of ionosphere variability associated with seismic activity from the one hand and from the other hand the properties which are not used often while they could be very useful in the precursors' identification such as the vertical profile scale height variations. But the main purpose of the paper was to give the clear demonstration how Global Electric Circuit works in transmitting information from the ground surface up to the ionosphere through the changing of its electrical properties due to natural ionization and ion induced nucleation changing the conductivity of the atmosphere column.

Acknowledgement

References

Astafyeva E.I. and Afraimovich E.L., Long-distance traveling ionospheric disturbances caused by the great Sumatra-Andaman earthquake on 26 December 2004, Earth Planets Space, 58, 1025–1031, 2006

BBC News, Volcanic ash: Flight chaos to continue into weekend. http://news.bbc.co.uk/2/hi/europe/8623534.stm , 16 April, 2010

Bowman D.D., Ouillon G., Sammis C.G., Sornette A. Sornette D., An observation test of the critical earthquake concept, J. Geophys. Res., 103, 24359-24372, 1998

Bradley P.A., Cander L.R., Proposed terminology for the classification and parameters for the quantification of variability in ionosphere morphology, Annals of Geophysics, 45, 97-104, 2002

Davidenko D.V., Diagnostics of ionospheric disturbances over the seismo-active regions, PhD Thesis, Fiodorov Institute of Applied Geophysics, Moscow, July, 2013, 147 p.

Dobrovolsky, I.R., Zubkov, S.I., Myachkin, V.I., Estimation of the size of earthquake preparation zones, Pageoph., 117, 1025-1044, 1979

Freund, F., Toward a unified solid state theory for pre-earthquake signals, Acta Geophys., 58(5), 719–766, doi:10.2478/s11600-009-0066-x, 2010.

Fuks M. Shubova R.S., Martynenko S.I., Lower ionosphere response to conductivity variations of the near-earth atmosphere, Journal of Atmospheric and Solar-Terrestrial Physics. 59, 961-965, 1997.

Galvan, D.A., Komjathy A., Hickey M.P., Stephens P., Snively J., Tony Song Y., Butala M.D., and Mannucci A.J. (2012), Ionospheric signatures of Tohoku-Oki tsunami of March 11, 2011: Model comparisons near the epicenter, Radio Sci., 47, RS4003, doi:10.1029/2012RS005023.

Gringel, W., and Mühleisen R., Sahara dust concentration in the troposphere over the North Atlantic derived from measurements of air conductivity, *Beitr. Phys. Atmos*. 51, 121-128, 1978.

Hayakawa M., Kasahara Y., Nakamura T., Muto F., Horie T., Maekawa S., Hobara Y., Rozhnoi A.A., Solovieva M., and Molchanov O.A., A statistical study on the correlation between lower ionospheric perturbations as seen by subionospheric VLF/LF propagation and earthquakes, J. Geophys. Res., 115, A09305, doi:10.1029/2009JA015143, 2010

Hirooka S., Hattori K.; Nishihashi M.; Takeda T., Neural network based tomographic approach to detect earthquake-related ionospheric anomalies, Natural Hazards and Earth System Science, 11(8):2341-2353, 2011.

Hoppel W.A., Anderson R.V., Willet J.C., Atmospheric Electricity in the Planetary Boundary Layer, in: The Earth's Electrical Environment, National Academic Press, Washington, DC, 149–165, 1986.

Hsiao C.-C., Liu J. Y., Oyama K.-I., Yen N. L., Liou Y. A., Chen S. S., Miau J. J., Seismo-ionospheric precursor of the 2008 Mw7.9 Wenchuan earthquake observed by FORMOSAT-3/COSMIC, GPS Solut. (2010) 14:83–89, DOI 10.1007/s10291-009-0129-0

Kathmann S.M., Schenter G.K., and Garrett B.C., Ion-Induced Nucleation: The Importance of Chemistry, Physical Review Letters, 94, DOI: 10.1103/PhysRevLett.94.116104, 2005

Kawabata H., Narita H., Harada K., Tsunogai S., Kasakabe M., Air-Sea Gas Transfer Velocity in Stormy Winter Estimated from Radon Deficiency, Journal of Oceanography, Vol. 59, pp. 651 to 661, 2003

Khilyuk L.F., Chillingar G.V., Robertson Jr. J.O., Endres B., 2000, Gas migration. Events preceding earthquakes, Gulf Publishing Company, Houston, Texas, 390 p.

Kim V. P., Hegai V. V., Illich-Svitych P. V., On one possible ionospheric precursor of earthquakes Physics of the Solid Earth 30: 223-226, 1994

Kim V.P., Pulinets S.A., Hegai V.V., Theoretical model of possible disturbances in the nighttime mid-latitude ionospheric D-region over an area of strong-earthquake preparation, Radiophysics and Quantum Radioelectronics (Izvestiya VUZov RADIOFIZIKA), 45, 262-268, 2002

Kim V. P., Liu J. Y., Hegai V. V., Modeling the pre-earthquake electrostatic effect on the F region ionosphere, Advances in Space Research, 50, 1524–1533, 2012.

Klimenko M. V., Klimenko V .V., Zakharenkova I. E., Pulinets S. A., Zhao B., Tzidilina M. N., Formation Mechanism of Great Positive Disturbances prior to Wenchuan earthquake on May 12, 2008, Advances in Space Research, 48, 488-499, 2011

Kunitsyn V., Nesterov I., Andreeva E., Rekenthaler D. A., Radio Tomography of Ionospheric Structures (probably) due to Underground-Surface-Atmosphere-Ionosphere Coupling, AGU Fall Meeting, San Francisco, USA, NH43C-06

Kuo C. L., Huba J. D., Joyce G., and Lee L. C., Ionosphere plasma bubbles and density variations induced by preearthquake rock currents and associated surface charges, Journal of Geophysical Research, 116, Article ID A10317, 2011.

Le, H., J. Y. Liu, and L. Liu (2011), A statistical analysis of ionospheric anomalies before 736 M6.0+ earthquakes during 2002–2010, J. Geophys. Res., 116, A02303, doi:10.1029/2010JA015781.

Li K.C., Feng J., Pan X. and Qu C.Y., Application of multi-parameter infrared remote sensing in seismic monitoring. International Workshop of Earthquake Anomaly Recognition. September 18–20, 2011, Northeastern University, Shenyang, China, 2011.

Li M. and Parrot M., Statistical analysis of an ionospheric parameter as a base for earthquake prediction, J. Geophys. Res., 2013, 118, 3731–3739, 2013

Liperovsky V.A., Meister C.-V., Liperovskaya E.V., Vasil'eva N.E., Alimov O., On spread - Es effects in the ionosphere before earthquakes, Natural Hazards and Earth System Sciences, 5, 59–62, 2005.

Liu, J.-Y., Y.-B. Tsai, K.-F. Ma, Y.-I. Chen, H.-F. Tsai, C.-H. Lin, M. Kamogawa, and C.-P. Lee, Ionospheric GPS total electron content (TEC) disturbances triggered by the 26 December 2004 Indian Ocean tsunami, J. Geophys. Res., 111, A05303, doi:10.1029/2005JA011200, 2006a

Liu, J. Y., Y. I. Chen, Y. J. Chuo, and C. S. Chen, A statistical investigation of preearthquake ionospheric anomaly, J. Geophys. Res., 111, A05304, doi:10.1029/2005JA011333, 2006b

Liu J.Y., Chen Y.I., Chen C.H., and K. Hattori, Temporal and spatial precursors in the ionospheric global positioning system (GPS) total electron content observed before the 26 December 2004 M9.3 Sumatra–Andaman Earthquake, J. Geophys. Res., 115, A09312, doi:10.1029/2010JA015313, 2010

Liu Z., Luo W., Ding X., Chen W., The New Characteristics of Ionospheric Total Electron Content (TEC) Disturbances prior to Four Large Earthquakes, "7th Annual seminar on Spatial Information Science and Technology (ASSIST 2011)", Hong-Kong, 2011

Mareev E.A., Global electric circuit research: achievements and prospects, *PHYS-USP*, 53 (5), 527–534, 2010.

Markson R., The global circuit intensity: its measurement and variation over the last 50 years. Bull. Am. Meteorol. Soc.. doi:10.1175/BAMS-88-2- 223, 223-241, 2007.

Masci F., Further comments on the ionospheric precursor of the 1999 Hector Mine earthquake, Nat. Hazards Earth Syst. Sci., 13, 193–196, 2013

Namgaladze A. A., Klimenko M.V., Klimenko V.V. and Zakharenkova I.E.. Physical Mechanism and Mathematical Modeling of Earthquake Ionospheric Precursors Registered in Total Electron Content. Geomagnetism and Aeronomy, 2009, v.49, No. 2, p. 252–262, 2009

Namgaladze A. A., Zolotov O. V., Karpov M. I., Romanovskaya Y. V., Manifestations of the earthquake preparations in the ionosphere total electron content variations, Natural Science Vol.4, No.11, 848-855, 2012, doi:10.4236/ns.2012.411113

Ouzounov, D., Pulinets S., Hattori K., Kafatos M., Taylor P., Atmospheric signals associated with major earthquakes. A multi-sensor approach, in "The Frontier of Earthquake Prediction Studies", Ed. by M. Hayakawa, Nihon-senmontosho-Shuppan, Tokyo, 510-531, 2012

Ouzounov D.P., Pulinets S.A., Davidenko D.A., Kafatos M., Taylor P.G., Space-borne observations of atmospheric pre-earthquake signals in seismically active areas. Case study for Greece 2008-2009, Thales, Special issue in honor of Prof. Emeritus Michael E. Contadakis, 1, 259-265, 2013

Park C. G., Dejnakarintra M. (1973) Penetration of thundercloud electric fields into the ionosphere and magnetosphere, 1. Middle and auroral latitudes. J. Geophys. Res. 84: 960-964

Parrot M., Li M., The use of an ionospheric parameter for earthquake prediction, paper NH44A-04, AGU Fall Meeting, San-Francisco, 3-7 December 2012

Pulinets S.A., Seismic activity as a source of the ionospheric variability, Adv. Space Res., 22, No 6, 903-906, 1998

Pulinets S. A., Physical mechanism of the vertical electric field generation over active tectonic faults, Advances in Space Research, 44, 767-773, 2009

Pulinets S., Low-Latitude Atmosphere-Ionosphere Effects Initiated by Strong Earthquakes Preparation Process, International Journal of Geophysics, vol. 2012, Article ID 131842, 14 pages, doi:10.1155/2012/131842, 2012.

Pulinets S. A., Khegai V. V., Boyarchuk K. A., Lomonosov A. M., The atmospheric electric field as a source of variability in the ionosphere, Physics-Uspekhi, 41, No 5, pp. 515-522, 1998a

Pulinets S.A., Legen'ka A.D., and Zelenova T.I., Local-Time Dependence of Seismo-Ionospheric Variations at the F-Layer Maximum, Geomagnetism and Aeronomy, 38, No.3, 400-402, 1998b

Pulinets S. A., Boyarchuk K. A., Hegai V. V., Kim V. P. and Lomonosov A. M., Quasielectrostatic Model of Atmosphere-Thermosphere-Ionosphere Coupling, Adv. Space Res., 26, No 8, pp.1209-1218, 2000

Pulinets S.A., Legen'ka A.D., Gaivoronskaya T.V., Depuev V.K., Main phenomenological features of ionospheric precursors of strong earthquakes. J. Atm. Solar Terr. Phys. 65, pp. 1337-1347, 2003

Pulinets S. A. and K. A. Boyarchuk, Ionospheric Precursors of Earthquakes, Springer, Berlin, Heidelberg, New York, 315 p., 2004.

Pulinets S.A., Biagi P., Tramutoli V., Legen'ka A.D., and Depuev V.Kh., Irpinia earthquake 23 November 1980 – Lesson from Nature revealed by joint data analysis, Annals of Geophysics, 50(1), 61-78, 2007a

Pulinets S.A., Kotsarenko N., Ciraolo L., and Pulinets I.A.: Special case of ionospheric day-to-day variability associated with earthquake preparation, Adv. Space Res., 39, 970–977, doi:10.1016/j.asr.2006.04.032, 2007b

Pulinets S.A., Bondur V.G., Tsidilina M.N., Gaponova M.V., Verification of the Concept of Seismoionospheric Relations under Quiet Heliogeomagnetic Conditions, Using the Wenchuan (China) Earthquake of May 12, 2008, as an Example, Geomagnetism and Aeronomy, 50, 231-242, 2010

Pulinets S., Ouzounov D., Lithosphere-Atmosphere-Ionosphere Coupling (LAIC) model - an unified concept for earthquake precursors validation, Journal of Asian Earth Sciences, 41, 371-382, 2011

Rozhnoi A., Solovieva M., Hayakawa M., Search for electromagnetic earthquake precursors by means of sounding of upper atmosphere-lower ionosphere boundary by VLF/LF signals, in The Frontier of Earthquake Prediction Studies, editor M. Hayakawa, Nihon-Senmontosho-Shuppan, 652-677, 2012

Rycroft M.J., Nicoll K.A., Aplin K.L., Harrison R.G., Recent advances in global electric circuit coupling between the space environment and the troposphere, *Journal of Atmospheric and Solar-Terrestrial Physics*, 90–91, 198–211, 2012

Smirnov V.M., Solution of the Inverse Problem of Electromagnetic Transmission Probing of the Earth Ionosphere by Gradient Methods, Journal of Communications Technology and Electronics, 46, 41-45, 2001

Sorokin V. M., Plasma and electromagnetic effects in the ionosphere related to the dynamics of charged aerosols in the lower atmosphere, Russian Journal of Physical Chemistry B, 1, No. 2, 138–170, 2007

Tammet H., Kulmala M., Simulation tool for atmospheric aerosol nucleation bursts, Aerosol Science, 36, 173–196, 2005

Toutain J.-P., Baubron J.-C., Gas geochemistry and seismotectonics: a review, Tectonophysics, 304, 1-27, 1998

Tertyshnikov A.V., Skripachev V.O., Chernyavskii G.M., Variations in deceleration of space vehicles in the upper ionosphere before strong earthquakes, Doklady Earth Sciences, 424, Issue 1, 180-184, 2009

Thomas J.N., Love J.J., Komjathy A., Verkhoglyadova O.P., Butala M., Rivera N., On the reported ionospheric precursor of the 1999 Hector Mine, California earthquake, Geophysical Research Letters, 39, L06302, doi:10.1029/2012GL051022, 2012

Williams E.R., The global electrical circuit: A review, *Atmospheric Research*, 91, 140–152, 2009

Xia, C., Wang Q., Yu T., Xu G., Yang S., Variations of ionospheric total electron content before three strong earthquakes in the Qinghai-Tibet region, Adv. Space Res., 47, 506-514, 2011

Zhang X., Shen X., Liu J., Ouyang X., Qian J., and Zhao S., Analysis of ionospheric plasma perturbations before Wenchuan earthquake, Nat. Hazards Earth Syst. Sci., 9, 1259–1266, 2009

Zolotov O.V., Namgaladze A.A., Zakharenkova I.E., Martynenko O.V., Shagimuratov I.I., Physical Interpretation and Mathematical Simulation of Ionospheric Precursors of Earthquakes at Midlatitudes, Geomagnetism and Aeronomy, 52, 413-420, 2012

Figure Captures

Figure 1. Relative variations $dTEC_{DOY}=TEC_{DOY}-TEC_{DOY-3}$ around the time of the Wenchuan M8 earthquake on 12 May 2008 (after Liu et al., 2011)

Figure 2. Occurrence rate of anomalies of R > 60%, 80%, and 100% within T days before earthquakes (PE) of depth ≤ 20, 30, and 40 km, respectively (after Le et al., 2011)

Figure 3. Upper panel – deviation of the critical frequency foF2 scaled from the topside ionograms of Intercosmos-19 satellite along the orbit passing over the preparation area of Irpinia M6.9 earthquake 23 Nov 1980; bottom panel - the differential GIM map over the area of preparation Sumatra Andaman M9.1 earthquake on 26 Dec 2004 (after Liu et al., 2010)

Figure 4. Left panel - the differential GIM map over the area of preparation of the M6.7 earthquake in Greece 8 Jan 2006; right panel – the global differential GIM map 3 days before Wenchuan M8 earthquake on 12 May 2008

Figure 5. Variations of the critical frequency foF2 (red) and sporadic E-layer critical frequency foE_S (blue) for the period 12 Aug – 12 Sept 2008 by the data of Irkutsk vertical ionospheric sounder

Figure 6. Upper panel – Concentration of H^+ ions registered onboard the DEMETER satellite over the area of Wenchuan M8 earthquake preparation for the period April-May 2008 (after Zhang et al., 2009); lower panel – variations of vertical profile of electron concentration semi-thickness over the epicenter of Wenchuan M8 earthquake for the period 27 Apr-13 May 2008

Figure 7. Variation of ionospheric potential Vi from 1955 to 2004. The number of balloon soundings used for each year are given. Lower curves show the nuclear deposition indicating radioactive Sr-90 fallout on the ground (green), while the stratospheric burden is a measure of Sr-90 in the stratosphere (black). Modified from Markson (2010)

Figure 8. Schematic diagram of the Global Electric Circuit

Figure 9. Left panel – the temporal sequence of diagrams showing the spatial distribution of ash deposited in atmosphere from the Eyjafjallajökull volcano on

16 Apr 2010; right panel – the differential GIM maps over Europe for 16-18 Apr 2010

Figure 10. Left panel – balloon profile of atmosphere conductivity during Sahara dust storm on 26 Nov 1973 (after Gringel and Mühleisen, 1978); right panel – the sequence of differential GIM maps during Sahara dust storm 1-2 May 2012

Figure 11. The differential GIM map collected 1 hour after the underground nuclear test in Northern Korea on 12 Feb 2013

Figure 12. Land surface temperature (LST) map registered by MODIS/Terra on May 1, 2008 (a) and on May 5, 2008 (b) (after Li et al., 2011)

Figure 13 a) – upper panel – Local Variability Index calculated using the data of local network of GPS receivers in California for period 1-31 Oct 1999 (after Pulinets et al., 2007b). Vertical Arrow indicates the moment of Hector Mine M7.1 earthquake on 16 Oct 1999; lower panel – the equatorial Dst index for the same time interval. b) left panel – 3D distribution of vertical GPS TEC over the area of preparation the Hector Mine M7.1 earthquake on 16 Oct 1999 13 Oct 1700; right panel – 3D distribution of vertical GPS TEC over the same area with the same set of receivers on 18 Oct 1700

Figure 14. a) upper panel - SSI calculated for period of 4 months before and during Sumatra Andaman M9.1 earthquake on 26 Dec 2004, lower panel – equatorial Dst index for the same period; b) upper panel – the seismic activity around the time of the Chile M8.8 earthquake on 27 Feb 2010, middle panel – the SSI calculated for period from 21 February till 19 March 2010, lower panel – the equatorial Dst index for the same period; c) upper panel – daily SSI from 05 March till 17 April 2009 calculated from GPS receivers network for L'Aquila M6.3 earthquake on 6 Apr 2009., lower panel – the daily Ap index of geomagnetic activity for the same period

(a)

Days

12.05.2008

Latitude/°

$Ni(H+)/cm^{-3}$

5000
4500
4000
3500
3000
2500
2000
1500
1000
500
0

(b)

Scale-height (km)

Date (2008)

Ionosphere   ~250 kV

R_i

ε ~

R_S

R_T Fair weather return current ~4 pA/m^2

R_{BL} E~100 V/m

Ground

Ascent at Pos. 16,5°N, 37°W
Launching 26.11.73 14.42 GMT

TECU